

Staphyloma II: Analyses of Morphological Features of Posterior Staphyloma in Pathologic Myopia Analyzed by a Combination of Wide-View Fundus Observation and 3D MRI Analyses

Kyoko Ohno-Matsui and Muka Moriyama

13.1 Introduction

In 1977, Curtin [1] classified a posterior staphyloma in eyes with pathologic myopia into ten different types. Types I to V are considered a primary staphyloma, and types VI to X are considered a combined staphyloma (see Staphyloma (I) of Chap. 13 for details). To date, this has been the most frequently used classification for staphyloma. Although this is a very useful classification, some improvements can be made. For example, this classification is based solely on ophthalmoscopic examination, and thus, the classification is rather subjective. Also, there are some types which are uncommon especially in the types of combined staphyloma, like type VI, VIII, or X. Finally, it is difficult to remember and routinely use as many as ten different types; thus, a simpler classification is needed.

Most of the staphyloma involves a wide area of the fundus; thus, the entire extent of staphyloma often does not fit within the 50° angle of the conventional fundus photos. Optical coherence tomography (OCT) is a useful tool for analyzing the curvature of the eye; however, the maximum scan length of commercially available OCT is not long enough to cover the entire extent of a wide staphyloma.

A relatively new technology, the Optos Optomap Panoramic 200A imaging system (Optos, PLC, Dunfermline, Scotland), combines both an ellipsoid mirror and a scanning laser ophthalmoscope (SLO) to obtain noncontact, nonmydriatic, panoramic fundus images. Optos allows for ultra-wide-field fundus imaging of nearly the entire retina (up

to 200°), during which the peripheral retina is captured simultaneously without the need for patient refixation.

Recently, we used three-dimensional magnetic resonance imaging (3D MRI) to analyze the entire shape of the eye [2, 3]. 3D MRI is considered suitable to analyze the eye shape of wide region like posterior staphyloma in a 3D way from any angle. There have been no studies analyzing how the entire eye looks like according to each type of staphyloma. It is also unclear whether the staphyloma affects the posterior eye segment only or it affects much broader range of the eye.

Thus, in this chapter, we propose a simple classification and examined the features of Optos images and 3D MRI images of the same individual. We also analyzed how the staphyloma seen in Optos images corresponds to the abnormal shape of the entire globe in 3D MRI images.

13.2 Principles for Classification of Staphyloma

1. *Only the contour of the outermost border of posterior staphyloma was analyzed:*

- Combined staphylomas in Curtin's classification [1] are characterized by the presence of irregularities within the staphylomatous area. However, recent enhanced depth imaging OCT (EDI-OCT) [4] and swept-source OCT have shown that there are more numerous and more complicated irregularities of the sclera within a staphyloma than expected earlier, such as dome-shaped macula [5–9], peripapillary intrachoroidal cavitation (ICC) [10], macular ICC [11], scleral dehiscence within patchy atrophy or at the emissary openings [12], change of scleral curvature at the dura attachment site [13], posterior protrusion of peripapillary sclera exposed onto the dilated subarachnoid space [13]. Thus, it is difficult to include many different kinds of scleral irregularities into the classification of staphyloma. From the

K. Ohno-Matsui, MD, PhD (✉) • M. Moriyama, MD, PhD
Department of Ophthalmology and Visual Science,
Tokyo Medical and Dental University, 1-5-45 Yushima,
Bunkyo-ku, Tokyo, 113-8510, Japan
e-mail: k.ohno.oph@tmd.ac.jp

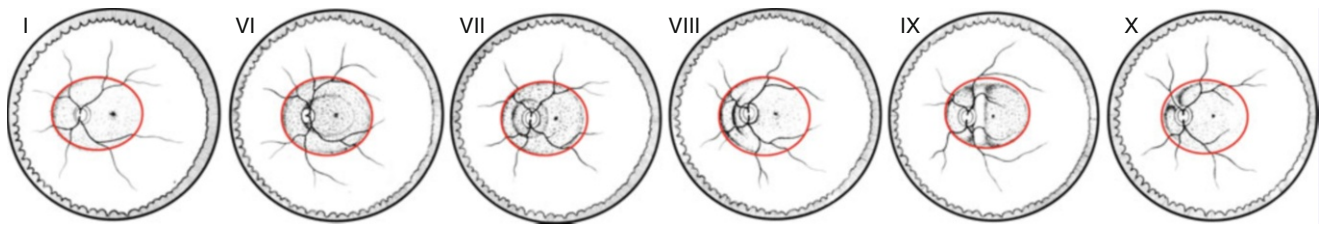


Fig. 13.1 The curvature of the outermost line of staphyloma is considered for a classification. The outermost line of staphyloma is depicted in red line. In such case, types VI through X fit into the same category of type I (in Curtin's classification)

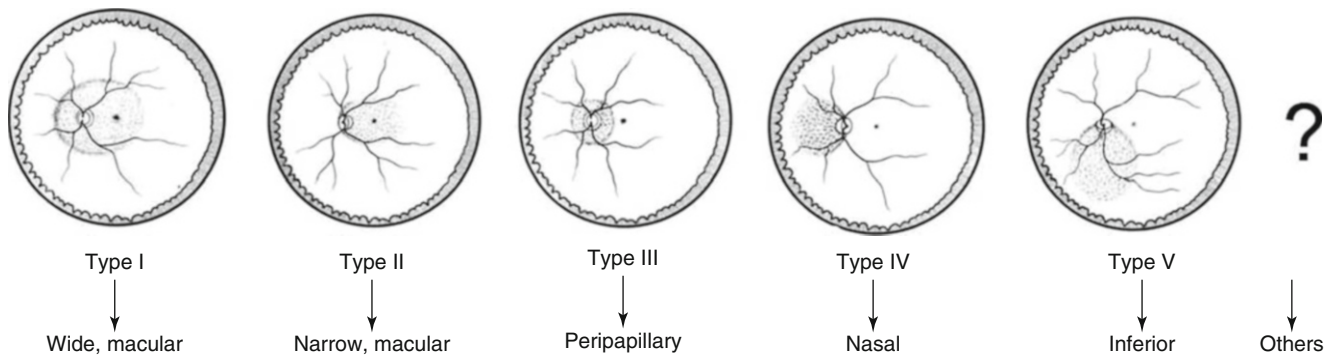


Fig. 13.2 Renaming of staphyloma according to its distribution

reasons above, we analyzed the outermost border only. That is, types VI to X are included under the same category with type I (Fig. 13.1).

2. *Staphyloma type is renamed according to its location and distribution* (Fig. 13.2):

- Type I → wide, macular staphyloma
- Type II → narrow, macular staphyloma
- Type III → peripapillary
- Type IV → nasal
- Type V → inferior
- Staphyloma other than type I through type V → others

13.3 Highly Myopic Eyes Without Evident Staphyloma (Fig. 13.3)

In Optos images, no clear abnormalities suggesting the staphyloma edge are found both in color images as well as fundus autofluorescence (FAF) images, although posterior fundus shows characteristic findings to pathologic myopia, such as myopic chorioretinal atrophy and myopic conus (Fig. 13.3a, e). 3D MRI images show an elliptical shape (Fig. 13.3c, e) or barrel shape (Fig. 13.3g, h) both in horizontal and vertical sections. Highly myopic eyes with longer axial length (especially >30.0 mm) tend to have barrel-shaped globe than elliptical shape when they do not have evident staphyloma.

13.4 Highly Myopic Eyes with Evident Staphyloma (Figs. 13.4, 13.5, 13.6, 13.7, 13.8, 13.9, 13.10, 13.11, and 13.12)

13.4.1 Macular Staphyloma

Macular staphyloma is further divided into wide and narrow, mainly due to a location of nasal edge of staphyloma. When the nasal edge of macular staphyloma is along the nasal edge of the optic disc, the eye is regarded as having a narrow, macular staphyloma. On the other hand, when the nasal edge of macular staphyloma exists more nasally to the nasal edge of the optic disc, the eye is considered as having a wide, macular staphyloma.

13.4.1.1 Wide, Macular Staphyloma (Fig. 13.4)

In the Optos images, the border of the staphyloma is observed as pigmented or depigmented lines in color images and as hypo-autofluorescent lines in FAF images in most cases. Generally, the upper and temporal border of the staphyloma is more clearly observed than the lower or nasal border. In some cases, band-shaped or tongue-shaped hypo-autofluorescent lesions surrounded by irregular hyper-autofluorescence seem to radiate outward from the border of staphyloma (arrows, Fig. 13.4b, j, n) in FAF images. This lesion shows pigmentation in color fundus (Fig. 13.4m);

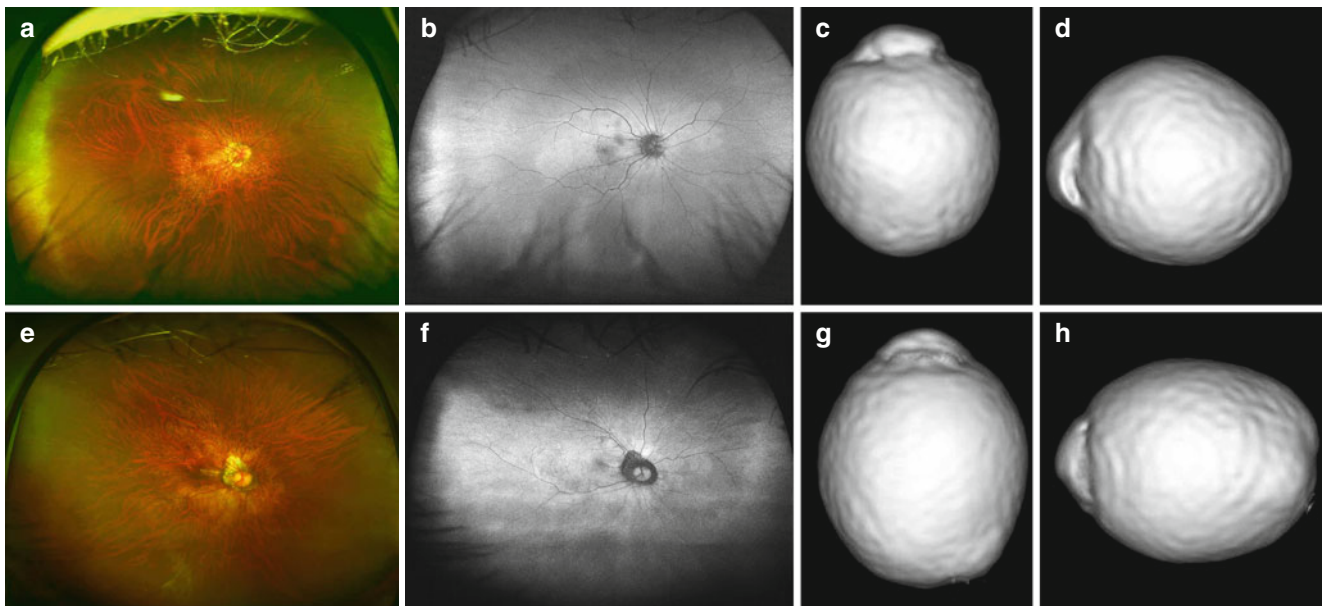


Fig. 13.3 Optos images and 3-dimensional magnetic resonance imaging (3D MRI) of highly myopic eyes without evident staphyloma. (a) Right fundus shows yellowish chorioretinal atrophy in the posterior fundus. Pigmentary abnormalities suggesting the border of staphyloma are not obvious. (b) Fundus autofluorescence (FAF) image shows no abnormal autofluorescence suggestive of border of staphyloma. (c, d) 3D MRI images of this patient. 3D MRI images of the right eye viewed from inferiorly (c) and the image viewed from nasally (d) show that the globe is elongated into an ellipsoid shape. No notch suggestive of an

abrupt change of the curvature of the globe is found. (e) Right fundus shows yellowish chorioretinal atrophy in the posterior fundus. Pigmentary abnormalities suggesting the border of staphyloma are not obvious. (f) Fundus autofluorescence (FAF) image shows no abnormal autofluorescence suggestive of border of staphyloma. (g, h) 3D MRI images of this patient. 3D MRI images of the right eye viewed from inferiorly (g) and the image viewed from nasally (h) show that the globe is elongated anterior-posteriorly and the globe shows a barrel-shaped appearance

however, this lesion is more clearly seen in FAF images than the color images.

3D MRI images show a protrusion of wide area of the posterior segment both in the images viewed from the inferior and nasal to the eye. Corresponding to the Optos images, the upper or temporal border is more abrupt than the lower or nasal border in the images viewed from nasally in most cases. Thus, there is a notch-like dent along the upper border of protrusion (arrows, Fig. 13.4d, p) or along the temporal border of the protrusion (Fig. 13.4c, k, o) in most cases. However, some cases have a notch along the lower border (Fig. 13.4i) or do not have obvious notch (Fig. 13.4h). Although all of the 3D MRI images viewed from inferiorly show a wide area of protrusion, in the 3D MRI images viewed from nasally, however, the size of protruded area are not wide in some eyes (Fig. 13.4i). This suggests that the staphyloma is horizontally wide in some of the eyes with wide, macular staphyloma.

In the images viewed from nasally, the most protruded point exists along the central visual axis in about 2/3 of the eyes and exists lower to the central axis in the remaining 1/3 (Moriyama 2013, unpublished data).

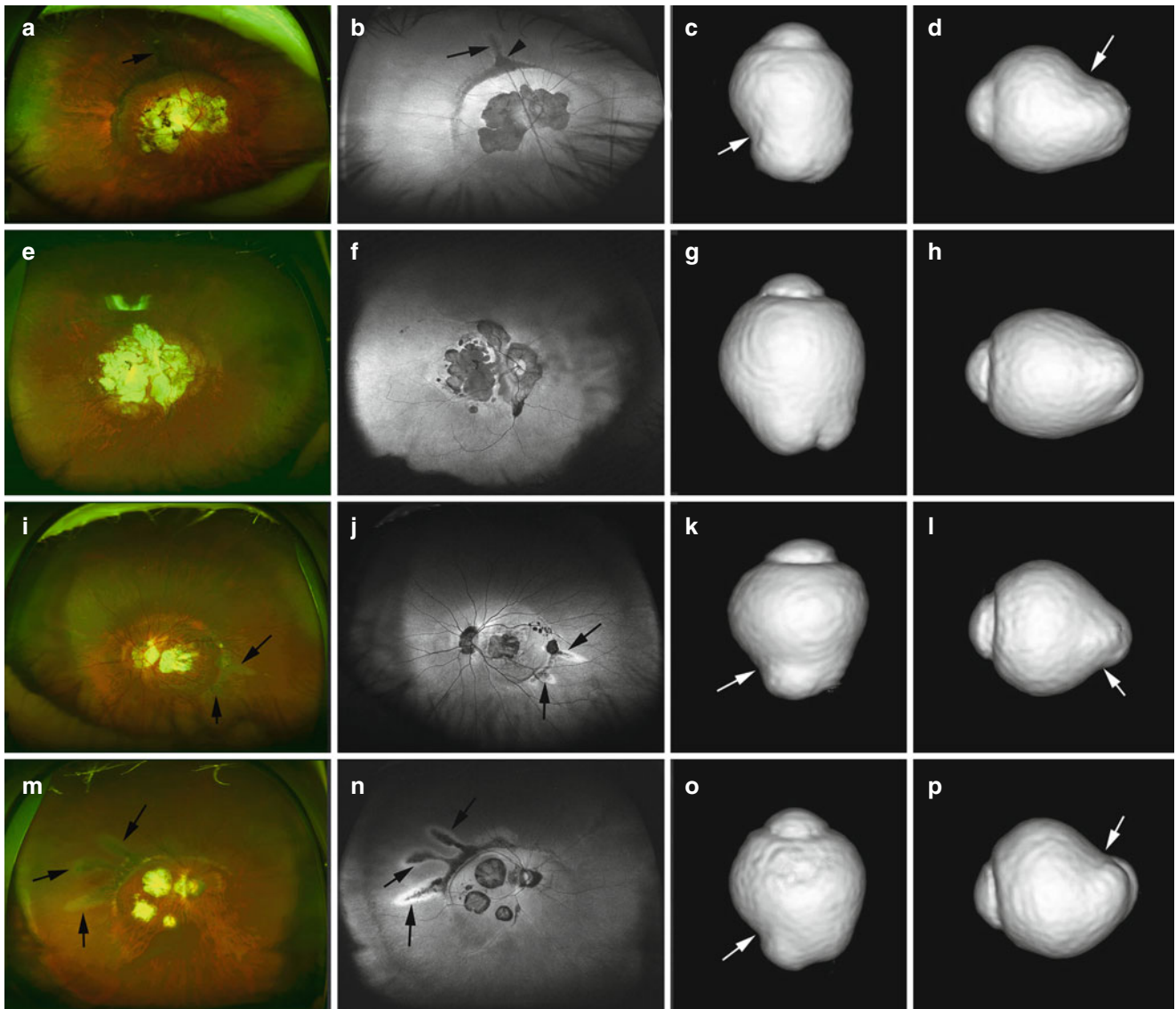
Scleral ridge formation temporal to the optic disc is a representative feature of type IX staphyloma by Curtin [1]. A ridge formation is the most frequently found in the

eyes with wide macular staphyloma among various types of staphyloma in Optos images. Actually, the ridge formation is more easily identified in 3D MRI images viewed from nasally (Fig. 13.4h, p) than Optos images. Even in eyes whose ridge formation is not obvious in Optos images, 3D MRI sometimes shows a presence of ridge.

Macroscopic image of a highly myopic eye with very wide staphyloma is shown in Fig. 13.5.

13.4.1.2 Narrow, Macular Staphyloma (Fig. 13.6)

In the Optos images, the area of protrusion is restricted to a narrow area from the nasal edge of the optic disc and temporal to the central fovea. Sometimes another small, shallow staphyloma is observed nasal to the optic disc (Fig. 13.6e, f). The border of staphyloma, especially upper and temporal border, shows pigmental abnormalities (Fig. 13.6a, e). FAF abnormalities along the border of staphyloma are not as remarkable as those seen in eyes with wide macular staphyloma, although FAF sometimes shows slight hyper-autofluorescence. In some cases, band-shaped abnormal FAF lesions radiating from the upper border of staphyloma is seen (Fig. 13.6f). However, this lesion is much less frequent and less evident than in eyes with wide, macular staphyloma.



3D MRI images show a “cylinder shape” which we previously reported [2]. Protruded area is narrow in the images viewed both from nasally and from inferiorly, and the protrusion of posterior segment seems to be pointed as a triangle, which is different from a broad and blunt protrusion seen in eyes with wide, macular staphyloma. In most of the eyes, the upper border is more acute than the lower border in the images viewed from nasally (Fig. 13.6d, h). However, the abruptness is milder than that in eyes with wild, macular staphyloma in general. And in the images viewed from inferiorly, the temporal border is more evident than the nasal border in most of the eyes (Fig. 13.6c); however, in some eyes, the nasal border is more evident (Fig. 13.6g). The most protruded point exists along the central axis in all of the eyes in the images viewed from nasally.

Macroscopic image of a narrow macular staphyloma is shown in Fig. 13.7.

13.4.2 Inferior Staphyloma (Fig. 13.8)

In the Optos images, the staphyloma exists in a wide area of lower fundus accompanying with myopic chorioretinal atrophy within a staphyloma. Optos images show that the upper border is clearly observed as pigmented line in color fundus images as well as hyper- or hypo-autofluorescent lines in FAF images (Fig. 13.8a, b). Some areas of the border of staphyloma show patchy areas of clear hypo-autofluorescence which suggests an atrophy of retinal pigmented epithelium. Band-shaped or tongue-shaped hypo-autofluorescent lesions

Fig. 13.4 Optos images and 3-dimensional magnetic resonance imaging (3D MRI) of highly myopic eyes with wide, macular staphyloma. (a) Right fundus shows a macular chorioretinal atrophy merged with myopic conus. The upper border of staphyloma is recognized as pigmented lines. (b) Fundus autofluorescence (FAF) image shows a hypo-autofluorescence along the upper edge of staphyloma. A band-shaped linear hypo-autofluorescent lesion is seen to course from the upper edge of staphyloma (*arrow*). An area with intense hypo-autofluorescence (*arrowhead*) is observed at the root of this band-shaped lesion. (c, d) 3D MRI images of this patient. 3D MRI image of the right eye viewed from inferiorly (c) shows that a wide area of posterior segment is protruded posteriorly. The temporal border of protrusion is more abrupt than the nasal border. Thus, a notch (*arrow*) is observed along the temporal border of protrusion. Protrusion of wide area of posterior segment is also seen in the 3D MRI image viewed from nasally (d). The upper border (*arrow*) seems to be more abrupt than the lower border. (e) Right fundus shows a macular chorioretinal atrophy merged with myopic conus. The border of staphyloma is slightly pigmented; however, the staphyloma edge is not as evident as the previous case. (f) FAF image shows no evident abnormalities along the border of staphyloma. (g, h) 3D MRI images of this patient. 3D MRI image of the right eye viewed from inferiorly (g) shows that a wide area of posterior segment is protruded posteriorly. Neither temporal nor nasal border of protrusion is abrupt. 3D MRI image of the right eye viewed from nasally (h) shows that a wide area of posterior segment is protruded posteriorly. Neither upper nor lower border of protrusion is abrupt. A ridge is observed within a protruded area in both images. (i) Left fundus shows a macular atrophy in the posterior fundus. The border of staphyloma is observed as pigmented line especially along the temporal border. Two linear lesions radiating from the temporal edge of staphyloma are seen

(*arrows*). (j) FAF image shows hypo-autofluorescence along the border of staphyloma (especially along the temporal border). Two hypo-autofluorescent linear lesions surrounded by irregular hyper-autofluorescence are shown to emanate from the temporal border of staphyloma (*arrows*). (k, l) 3D MRI images of this patient. 3D MRI image of the right eye viewed from inferiorly (k) shows that a wide area of posterior segment is protruded posteriorly. Temporal border is more abrupt than the nasal border; thus, a notch is observed along the temporal border of protrusion. 3D MRI image viewed from nasally (l) shows that protruded area is not as wide as that seen in the image viewed from inferiorly, suggesting a protrusion in this patient is horizontally wide. The lower edge seems to be more abrupt than the upper edge, and a notch is found along the lower edge (*arrow*). (m) Right fundus shows areas of chorioretinal atrophic patches in the posterior fundus. The border (especially upper border) of staphyloma shows pigmentation. Three pigmented linear lesions (*arrows*) are seen to radiate from the upper-temporal edge of staphyloma. A ridge formation temporal to the optic disc is observed. (n) FAF image shows hypo-autofluorescence along the border of staphyloma (especially along the upper border). Three hypo-autofluorescent linear lesions surrounded by irregular hyper-autofluorescence are seen to emanate from the upper-temporal border of staphyloma (*arrows*). (o, p) 3D MRI images of this patient. 3D MRI image of the right eye viewed from inferiorly (o) as well as the image viewed from nasally (p) show that a wide area of posterior segment is protruded posteriorly. Temporal border is more abrupt than the nasal border; thus, a notch is observed along the temporal border of protrusion in (o). Also, the upper edge seems to be more abrupt than the lower edge, and a notch is found along the upper edge (*arrow*). A ridge formation is observed as a linear groove within a protrusion

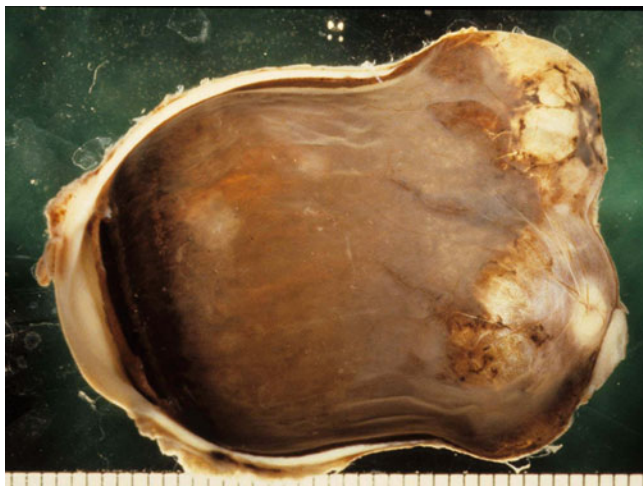


Fig. 13.5 Macroscopic view of a highly myopic eye with big multiple protrusions in wide, macular staphyloma. Both peripapillary and macular regions are posteriorly protruded. An extensive chorioretinal atrophy is seen in the entire posterior fundus. Axial length of the globe is 37 mm (Courtesy of Emeritus Professor Shigekuni Okisaka in National Defense Medical College)

surrounded by irregular hyper-autofluorescence are sometimes seen to radiate from the upper or temporal border of staphyloma (Fig. 13.8b). 3D MRI images of the eye with inferior staphyloma show a protrusion of lower segment of

the eye. Because an area of protrusion affects as widely as entire lower half of the globe (Fig. 13.8d), the lower boundary of protrusion is not obvious, and the curvature of the protrusion is gradually continuous to the curvature of the other parts of a lower half of the globe. The most protruded point exists lower to the central axis in the images viewed from nasally.

13.4.3 Peripapillary Staphyloma (Fig. 13.9)

In the Optos images, the boundary of peripapillary staphyloma is usually not obvious in color fundus images as well as FAF images, probably because the change of eye curvature is not abrupt. However, yellowish diffuse atrophy is seen especially around the optic disc (Fig. 13.9a), and we can see the depigmented demarcation line around the optic disc along the border of peripapillary staphyloma in some cases. The 3D MRI analyses show a protrusion of a limited area around the optic nerve attachment site in an image viewed from inferiorly. In the image viewed from nasally, the eye shape is similar to cylinder type which is observed in eyes with narrow, macular staphyloma; however, the area of protrusion tends to be more restricted around the optic nerve. The change of eye curvature toward the protrusion is relatively linear, and the posterior

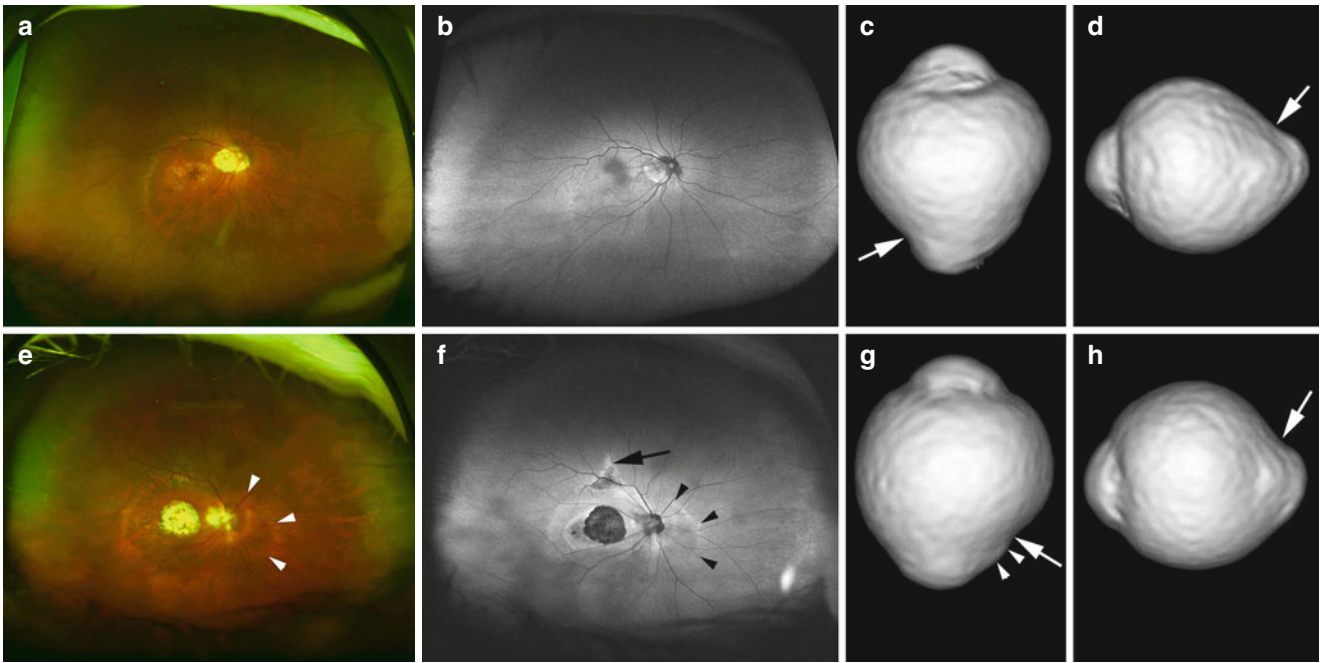


Fig. 13.6 Optos images and 3-dimensional magnetic resonance imaging (3D MRI) of highly myopic eyes with narrow, macular staphyloma. (a) Right fundus shows a narrow area of staphyloma. The upper and temporal border of staphyloma shows a slight depigmentation. Nasal edge of the staphyloma is along the nasal edge of the optic disc, and the optic disc shows a tilted appearance. (b) Fundus autofluorescence (FAF) imaging shows no abnormal autofluorescence suggestive of border of staphyloma. (c, d) 3D MRI images of this patient. 3D MRI image of the right eye viewed from inferiorly (c) as well as the image viewed from nasally (d) show that a protruded area is narrow and the protrusion of posterior segment seems to be pointed as a *triangle*. The temporal border is more abrupt than the nasal border (c, *arrow*), and the upper border is more acute than the lower border (d, *arrow*). The most protruded point exists along the central axis in all of the eyes in the images viewed from nasally. (e) Right fundus shows a narrow area of staphyloma. The upper and temporal border of staphyloma shows a slight

depigmentation. Nasal edge of the staphyloma is along the nasal edge of the optic disc, and the optic disc shows a tilted appearance. In this patient, another small staphyloma is also seen nasal to the optic disc (*arrowheads*). (f) FAF image shows slight hyper-autofluorescence along the border of staphyloma (*arrowheads*). A short linear hypo-autofluorescent lesion surrounded by hyper-autofluorescence is seen to emanate from the upper border of staphyloma (*arrow*). (g, h) 3D MRI images of this patient. 3D MRI image of the right eye viewed from inferiorly (g) as well as the image viewed from nasally (h) show that a protruded area is narrow and the protrusion of posterior segment seems to be rather pointed. The nasal border is more abrupt than the temporal border (g, *arrow*) in the image viewed from inferiorly. Small additional staphyloma nasal to the optic disc is also identified (*arrowheads*). The upper border is more acute than the lower border (h, *arrow*). The most protruded point exists along the central axis in all of the eyes in the images viewed from nasally



Fig. 13.7 Macroscopic view of a highly myopic eye with narrow, macular staphyloma. Macular area is posteriorly protruded and the sclera is extremely thinned in the protruded area. Axial length of the globe is 29 mm (Courtesy of Emeritus Professor Shigekuni Okisaka in National Defense Medical College)

pole of the eye seems to be protruded like a triangle (Fig. 13.9c).

Macroscopic view of an eye with peripapillary staphyloma is shown in Fig. 13.10. Note that the area around the optic nerve is specifically protruded, and the subsequent atrophy of retina-choroid is seen in the peripapillary region.

13.4.4 Nasal Staphyloma (Fig. 13.11)

In the Optos images, the boundary of nasal staphyloma is usually not obvious in most cases. However, yellowish diffuse atrophy is seen nasal to the optic disc, together with the nasal tilting of the optic disc as well as nasal conus. In some cases, the band-shaped line with abnormal autofluorescence is seen to course in parallel to the orientation of eye expansion away from the staphyloma border (Fig. 13.11b). Although the overall shape of the eye by 3D MRI is similar to that of peripapillary staphyloma, the protruded area is

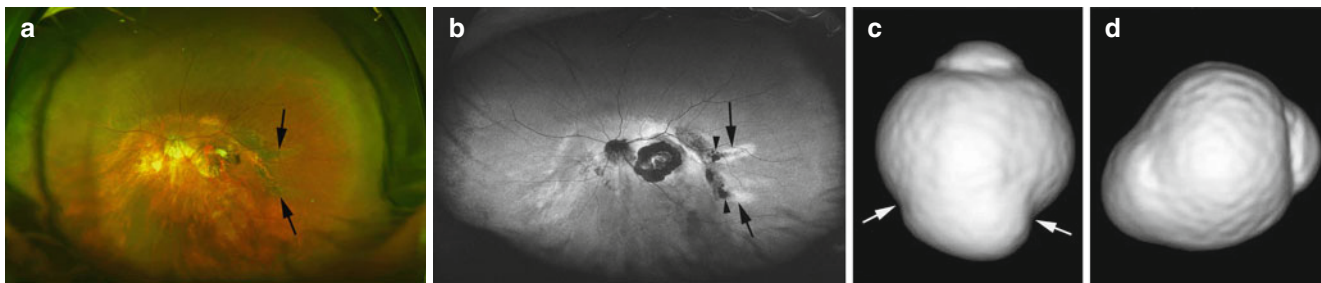


Fig. 13.8 Optos images and 3-dimensional magnetic resonance imaging (3D MRI) of a highly myopic eye with inferior staphyloma. (a) Left fundus shows an inferior staphyloma. The optic disc is tilted inferiorly and the inferior conus is seen. Macular atrophy is also seen. The upper border of inferior staphyloma shows pigmentation especially at the upper-temporal to temporal edge. Two linear lesions emanating from the temporal edge of staphyloma are observed (arrows). (b) Fundus autofluorescence image shows a hypo-autofluorescence corresponding to the pigmentation along the upper-temporal to temporal edge of staphyloma. Other parts of the upper border of staphyloma show slight hyper-fluorescence. Two linear lesions are seen to emanate from the

temporal border of staphyloma (arrows). The upper one has hyper-autofluorescence in the center of the line and the outside is surrounded by hyper-autofluorescence. The lower lesion shows hyper-autofluorescence. At the bottom of these linear lesions, an intense hypo-autofluorescence is observed (arrowheads). (c, d) 3D MRI images of this patient. 3D MRI image viewed from inferiorly (c) shows a protrusion of wide area. A notch is observed both along the temporal and nasal edge of protrusion (arrows). In the image viewed from nasally (d), the protrusion is decentered toward inferiorly. The lower border of protrusion is gradually continuous to the other parts of the eye; thus, the border between the protrusion and the other parts of the eye is not obvious

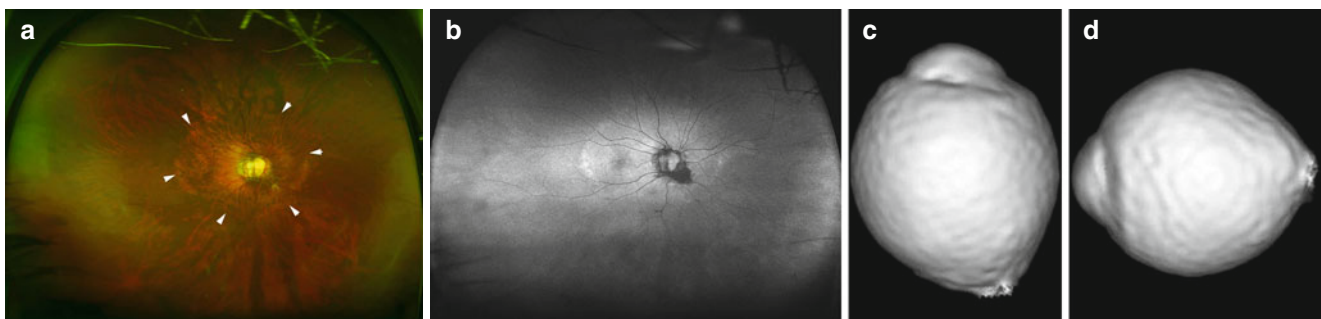


Fig. 13.9 Optos images and 3-dimensional magnetic resonance imaging (3D MRI) of a highly myopic eye with peripapillary staphyloma. (a) Right fundus shows a border of peripapillary staphyloma as slight depigmentation (arrowheads). (b) Fundus autofluorescence image shows a slight hyper-autofluorescence corresponding to the pigmentation along the temporal edge of staphyloma. (c, d) 3D MRI images of

this patient. 3D MRI image viewed from inferiorly (c) shows a protrusion of a limited area around the optic nerve attachment site. In the image viewed from nasally (d), the eye shape is similar to cylinder type; however, the area of protrusion tends to be more restricted. The change of eye curvature toward the protrusion is relatively linear, and the posterior pole of the eye seems to be protruded like a triangle



Fig. 13.10 Macroscopic view of a highly myopic eye with peripapillary staphyloma. The peripapillary region is posteriorly protruded, and the optic nerve is situated at the bottom of the protruded area. The sclera is extremely thinned in the protruded area. Axial length of the globe is 28 mm (Courtesy of Emeritus Professor Shigekuni Okisaka in National Defense Medical College)

wider, and the change of curvature is more gradual. Thus, the curvature of the posterior pole of the eye is more curvilinear than triangular.

13.4.5 Others

13.4.5.1 Peripapillary, Wide (Fig. 13.12)

Peripapillary staphyloma is generally seen just around the optic nerve. However, peripapillary staphyloma sometimes becomes wide and includes the central fovea. In Optos images, different from typical peripapillary staphyloma, the staphyloma is sometimes not concentrically around the optic disc. The temporal edge of the staphyloma is obliquely across the central fovea (Fig. 13.12). 3D MRI images show similar features to those of peripapillary staphyloma; however, a protrusion is wider than typical peripapillary staphyloma (Fig. 13.12b).

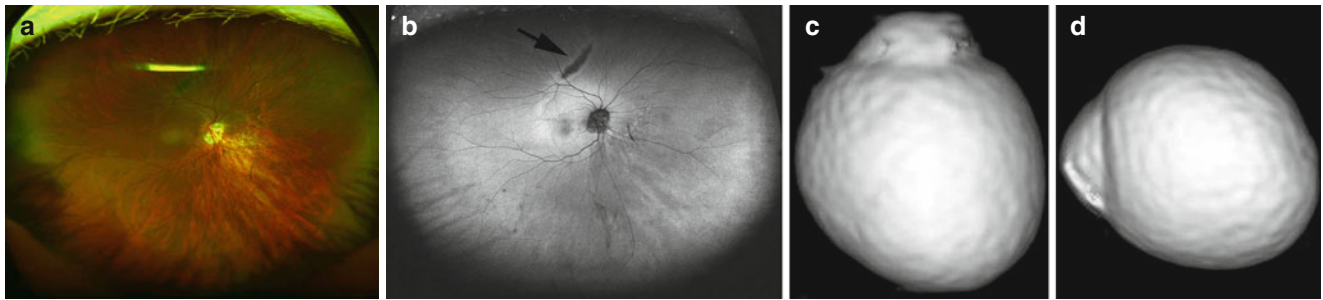


Fig. 13.11 Optos images and 3-dimensional magnetic resonance imaging (3D MRI) of a highly myopic eye with nasal staphyloma. (a) Right fundus shows an ectasia of nasal fundus. The optic disc is tilted nasally and accompanies with nasal conus. Yellowish diffuse atrophy is seen nasal to the optic disc. No obvious findings suggestive of a border of staphyloma are observed. (b) Fundus autofluorescence image shows no obvious abnormalities suggestive of staphyloma. A linear hypoautofluorescent lesion surrounded by a margin of hyper-fluorescence (*arrow*) is seen in the upper fundus away from the nasal staphyloma.

The orientation of this linear lesion seems parallel to the nasal tilting. (c, d) 3D MRI images of this patient. 3D MRI image viewed from inferiorly (c) shows a protrusion of nasal part of the eye, and the image viewed from nasally (d) shows a protrusion of the lower part of the eye. Although the overall shape of the eye by 3D MRI is similar to that of peripapillary staphyloma, the protruded area is wider, and the change of curvature is more gradual. Thus, the curvature of the posterior pole of the eye is more curvilinear than triangular

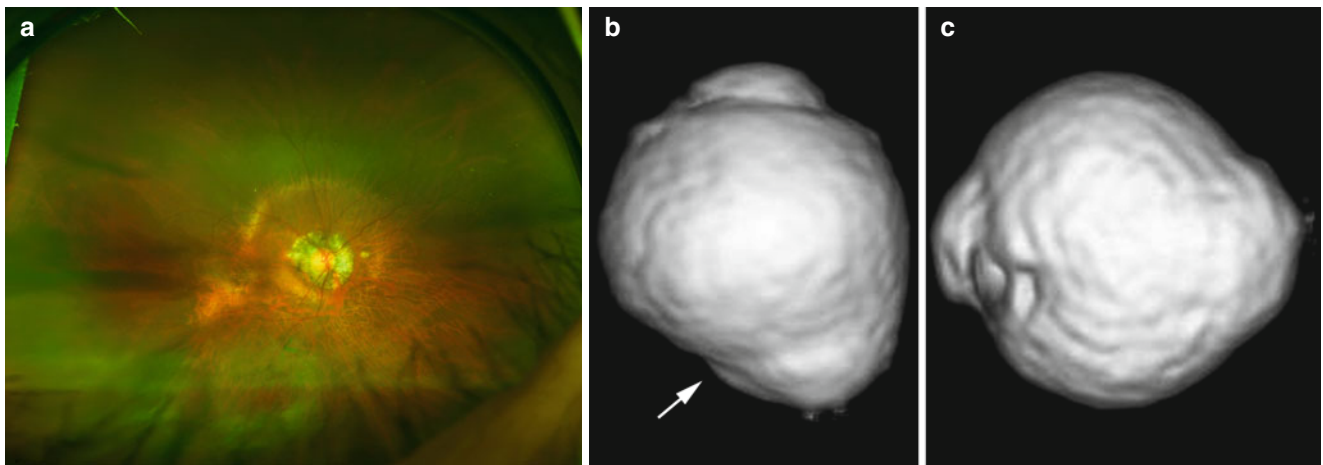


Fig. 13.12 Optos images and 3-dimensional magnetic resonance imaging (3D MRI) of a highly myopic eye with "other" type of staphyloma. (a) Right fundus shows a fundus ectasia involving around the optic disc as well as the lower fundus. The temporal border of staphyloma is obliquely across the central fovea (b, c) 3D MRI images of this patient. 3D MRI image viewed from inferiorly (b) shows a protrusion

of nasal part of the eye. The image viewed from nasally (c) shows that a protrusion exists along the central axis. Although the overall shape of the eye by 3D MRI is similar to that of peripapillary staphyloma, the protruded area is wider. A notch is found along the temporal edge of staphyloma (*arrow*, b)

13.5 Comments

A combination of Optos and 3D MRI is useful to delineate the entire extent of posterior staphyloma in a 3D way. 3D MRI images show various distinct features according to the types of staphyloma identified by Optos. In Optos images, the border of staphyloma is more clearly seen as pigmentary abnormalities in eyes with wide, macular staphyloma or inferior staphyloma, than the other types of staphyloma. Even in the eyes with wide, macular staphyloma, the upper and temporal borders are more clearly recognized.

In the 3D MRI images viewed from nasally, the upper border of protrusion is more abrupt than the lower border in eyes with wide, macular staphyloma. These suggest that in eyes with wide, macular staphyloma, the change of eye curvature is more acute and abrupt along the upper and temporal border than the lower and nasal border. The boundary of staphyloma is clearly observed as pigmentary changes in color fundus and FAF abnormalities mostly in eyes with wide, macular staphyloma and those with inferior staphyloma. In contrary, the eyes with other types of staphyloma (narrow macular, peripapillary, nasal) did not show obvious abnormalities at the border of staphyloma in general.

The cause of different FAF abnormalities along the border of staphyloma among different types is unclear. Although no measurements were made, there is a tendency that the wider the staphyloma, the deeper the staphyloma is. Thus, one possibility is that wide, macular staphyloma or inferior staphyloma might be deeper, and thus, the border (especially the upper border) might be more acute (like a cliff) than the other types of staphyloma.

The fact that the most protruded point exists along the central axis in all of the eyes with narrow, macular staphyloma but exists lower to the central axis in most of the eyes with wide, macular staphyloma suggests that the protrusion occurs along the central axis when the protruded area is small. And then, when a staphyloma becomes wider, the lower area of the posterior segment tends to be protruded more for unknown reason.

By 3D MRI, the area of protrusion is wide in eyes with wide, macular, or inferior staphyloma, whereas the protruded area is restricted in narrow, macular, peripapillary, or nasal staphyloma. In the inferior staphyloma, the deformity of lower eye segment is so wide that no boundary between the lower edge of staphyloma and the other parts of the eye is not clear. In contrary, in the wide, macular staphyloma, the boundary between the lower edge of staphyloma and the other parts of the eye can be recognized, even though the staphyloma seems very wide.

The band-shaped and tongue-shaped lesions with abnormal FAF are observed to radiate from the staphyloma edge mainly in eyes with wide, macular staphyloma and in inferior staphyloma in some cases. The color fundus findings as well as FAF features of these lesions are similar to those of the “atrophic tract” which is seen in eyes with central serous chorioretinopathy [14]. Some of these lesions show a presence of subretinal fluid by OCT (unpublished data). Although the pathology and cause of these lesions are unclear, it seems that these lesions are related to the serious damage of the retinal pigment epithelium at the border of staphyloma with abrupt margin (thus, upper or temporal border). Also, the orientation of the eye expansion may influence the development and course of this lesion (Fig. 13.11b).

In eyes with inferior staphyloma, the upper edge of staphyloma which goes across the central fovea shows pigmentary abnormalities and subsequent visual disturbance. Maruko et al. [15] found that the subfoveal sclera along the upper edge of inferior staphyloma was significantly thickened than the sclera upper and lower to the fovea, which was interestingly similar to that found in dome-shaped macula by Imamura and Spaide [6]. In addition to the pigmentary alterations of the staphyloma border itself, chorioretinal folds and

tongue-shaped FAF abnormalities are also seen to emanate from the upper edge of staphyloma toward upper periphery.

It is expected that there will be a lot more variations in “other” types of staphyloma. The studies including a larger population of patients are necessary to clarify the entire figure of staphyloma.

References

1. Curtin BJ. The posterior staphyloma of pathologic myopia. *Trans Am Ophthalmol Soc.* 1977;75:67–86.
2. Moriyama M, Ohno-Matsui K, Hayashi K, et al. Topographical analyses of shape of eyes with pathologic myopia by high-resolution three dimensional magnetic resonance imaging. *Ophthalmology.* 2011;118(8):1626–37.
3. Moriyama M, Ohno-Matsui K, Modegi T, et al. Quantitative analyses of high-resolution 3D MR images of highly myopic eyes to determine their shapes. *Invest Ophthalmol Vis Sci.* 2012;53(8):4510–8.
4. Margolis R, Spaide RF. A pilot study of enhanced depth imaging optical coherence tomography of the choroid in normal eyes. *Am J Ophthalmol.* 2009;147(5):811–5.
5. Gaucher D, Erginay A, Lecleire-Collet A, et al. Dome-shaped macula in eyes with myopic posterior staphyloma. *Am J Ophthalmol.* 2008;145(5):909–14.
6. Imamura Y, Iida T, Maruko I, et al. Enhanced depth imaging optical coherence tomography of the sclera in dome-shaped macula. *Am J Ophthalmol.* 2011;151(2):297–302.
7. Pardo-Lopez D, Gallego-Pinazo R, Mateo C, et al. Serous macular detachment associated with dome-shaped macula and tilted disc. *Case Report Ophthalmol.* 2011;2(1):111–5.
8. Coco RM, Sanabria MR, Alegria J. Pathology associated with optical coherence tomography macular bending due to either dome-shaped macula or inferior staphyloma in myopic patients. *Ophthalmologica.* 2012;228(1):7–12.
9. Jonas JB, Jonas SB, Jonas RA, et al. Parapapillary atrophy: histological gamma zone and delta zone. *PLoS One.* 2012;7(10):18.
10. Spaide RF, Akiba M, Ohno-Matsui K. Evaluation of peripapillary intrachoroidal cavitation with swept source and enhanced depth imaging optical coherence tomography. *Retina.* 2012;32:1037–44.
11. Ohno-Matsui K, Akiba M, Moriyama M, et al. Intrachoroidal cavitation in macular area of eyes with pathologic myopia. *Am J Ophthalmol.* 2012;154:382–93.
12. Ohno-Matsui K, Akiba M, Moriyama M, et al. Acquired optic nerve and peripapillary pits in pathologic myopia. *Ophthalmology.* 2012;119(8):1685–92.
13. Ohno-Matsui K, Akiba M, Moriyama M, et al. Imaging the retrobulbar subarachnoid space around the optic nerve by swept source optical coherence tomography in eyes with pathologic myopia. *Invest Ophthalmol Vis Sci.* 2011;52:9644–50.
14. Imamura Y, Fujiwara T, Spaide RF. Fundus autofluorescence and visual acuity in central serous chorioretinopathy. *Ophthalmology.* 2011;118(4):700–5.
15. Maruko I, Iida T, Sugano Y, et al. Morphologic choroidal and scleral changes at the macula in tilted disc syndrome with staphyloma using optical coherence tomography. *Invest Ophthalmol Vis Sci.* 2011;52(12):8763–8.